ChemBioChem

Research Article
doi.org/10.1002/cbic.202400024

Chemistry Europe
European Chemical Societies Publishing

www.chembiochem.org

Thermal Proteome Profiling Reveals Insight to Antiproliferative and Pro-Apoptotic Effects of Lagunamide A in the Modulation of DNA Damage Repair

Yudong Hu[+],[a] Dietrich Mostert[+],[b] Christina Orgler,[a] Oliver Andler,[c] Hans Zischka,[d, e] Uli Kazmaier,[c] Angelika M. Vollmar,[a] Simone Braig,[a] Stephan A. Sieber,*[b] and Stefan Zahler*[a]

Lagunamide A is a biologically active natural product with a yet unidentified molecular mode of action. Cellular studies revealed that lagunamide A is a potent inhibitor of cancer cell proliferation, promotes apoptosis and causes mitochondrial dysfunction. To decipher the cellular mechanism responsible for these effects, we utilized thermal protein profiling (TPP) and identified EYA3 as a stabilized protein in cells upon lagunamide A treatment. EYA3, involved in the DNA damage repair process, was functionally investigated via siRNA based knockdown studies and corresponding effects of lagunamide A on DNA repair were confirmed. Furthermore, we showed that lagunamide A sensitized tumor cells to treatment with the drug doxorubicin highlighting a putative therapeutic strategy.

Introduction

Lagunamide A (Lag A) and its analogues lagunamides B and C are potent cyclic depsipeptides obtained from the marine cyanobacterium Lyngbya majuscule.[1] These molecules are structurally related to a series of other cytotoxic marine cyanobacterial compounds, which can be subsumed in the aurilide family of compounds, which are already known to exhibit pronounced anticancer effects.[2] Previous studies described potent growth inhibitory activities of lagunamides in the low nanomolar range against a panel of cancer cell lines.[2–3] Furthermore, first biochemical studies of Lag A revealed that the cytotoxic effect of the natural compound is triggered via mitochondria-mediated apoptosis.[4] Thus, it seems that the structural similarity between aurilide and lagunamide, and their similar modes of action might be related. For aurilide. the mitochondrial protein prohibitin has been proposed as molecular target in an affinity based approach.[5] However, target identification studies for Lag A are still lacking. Given the need for novel targets in cancer therapy, strategies to unravel the mode of action of potent natural products are of major importance.

Identifying the molecular target of a drug is still challenging, especially, when chemically complex natural compounds are taken into consideration. An attractive strategy is affinity-based proteome profiling (AfBPP) to directly identify target proteins of a natural product in an unbiased manner.[6] However, this technique requires chemical alteration of the core scaffold in order to introduce affinity and photoreactive groups, which can be associated with reduced binding affinity to the respective target. Alternative methods such as thermal proteome profiling (TPP) determine changes in protein stability upon binding of the unmodified natural product.[7] Proteins which are stabilized via compound binding remain soluble at elevated temperatures and can thus be determined in the mass-spectrometric analysis of compound treated vs. untreated proteomes. We have recently used this method to identify the target of the natural compound vioprolide A where AfBPP was unsuccessful.[8]

[a] Dr. Y. Hu,[+] Dr. C. Orgler, Prof. A. M. Vollmar, Dr. S. Braig, Prof. S. Zahler
Department of Pharmacy
Ludwig-Maximilians-University
Butenandtstr. 5, 81377 Munich, Germany
E-mail: Stefan.zahler@cup.uni-muenchen.de

[b] D. Mostert,[+] Prof. S. A. Sieber
Center for Functional Protein Assemblies (CPA), Department of Chemistry,
Chair of Organic Chemistry II
Technical University of Munich
85748 Garching, Germany
E-mail: stephan.sieber@tum.de

[c] Dr. O. Andler, Prof. U. Kazmaier
Organic Chemistry
Saarland University
66123 Saarbrücken, Germany

[d] Prof. H. Zischka
Institute of Molecular Toxicology and Pharmacology
Helmholtz Center Munich, German Research Center for Environmental Health
Neuherberg, Germany

[e] Prof. H. Zischka
Institute of Toxicology and Environmental Hygiene
Technical University of Munich
Munich, Germany

[+] These authors contributed equally.

Supporting information for this article is available on the WWW under https://doi.org/10.1002/cbic.202400024

However, changes in protein-protein-interactions[9] or posttranslational modifications[10] can also change the thermal stability of a protein, which means that downstream effects of compound treatment will also be visible when performing the experiments in living cells.

We here utilize in depth proteome profiling by AfBPP and TPP to search for a protein target of Lag A. Functional assays demonstrate mitochondrial effects and a pro-apoptotic action. While we were not able to propose a direct mitochondrial target, we identify the transcriptional coactivator and phosphatase EYA3 as a part of the molecular mechanism underlying the pro-apoptotic action of Lag A and its effect on the DNA damage response.

Experimental Section

Cell Lines and Reagents

HeLa (derived from a 31-year-old female) cells were obtained from the DSMZ and grown in DMEM (PAN Biotech, Cat# AC-LM-0012) supplemented with 10% fetal bovine serum (FBS, PAN Biotech, Cat# AC-SM-0027). S-Jurkat cells which were derived from the peripheral blood of a 14-year-old boy, were kindly provided by P. H. Krammer (DKFZ, Heidelberg, Germany) and cultivated in RPMI 1640 (PAN Biotech, Cat# P0416500) containing 10% FBS, 100 U/ml penicillin and 100 μg/ml streptomycin (PAN Biotech, Cat# P0607100) with additional 1 mM pyruvate (Merck, Cat# P5280). Both cell lines were cultured at 37 °C with 5% CO_2 in a humidified incubator. For gene silencing, cells were transfected with ON-TARGETplus Human EYA3 siRNA according to the manufacturer's instructions and ON-TARGETplus non-targeting control siRNA (nt siRNA) served as control. Briefly, HeLa cells were seeded in 6-well plates at a density of 0.42 million cells/well one day before transfection. 9 μL lipofectamine RNAiMAX transfection reagent and 0.1 μM siRNA were diluted in 150 μL opti-MEM medium (Thermo Fisher Scientific, Cat# 31985070) respectively and mixed gently and then incubated for 5 min. siRNA solution was added into transfection reagent solution followed by a gentle mix and incubated for 15 min at room temperature (RT) before adding dropwise to HeLa cells. Following transfection, expression of EYA3 was determined with Western Blot using the EYA3 antibody.

Treatment of Cells with Compounds

Cells were seeded the night before treatment. DMSO solution was diluted in the corresponding culture medium and did not exceed 0.1% (v/v) in all experiments. Cells were incubated with compounds at indicated concentrations and time points.

Cell Proliferation Assay

Crystal violet staining assay and CellTiter Blue (CTB) assay were performed to detect the effect of Lag A on cell proliferation in HeLa cells and Jurkat cells respectively. For the crystal violet staining assay, HeLa cells were seeded in 96-well plates at a density of 2500 cells/well the night before treatment and incubated with indicated concentrations of Lag A or DMSO. After 72 h, the medium was discarded and cells were washed with PBS and then stained with crystal violet solution (0.5% crystal violet, 20% methanol) for 10 min. Then cells were gently washed with water and dried followed by dissolving in sodium citrate solution (0.1 M sodium citrate, 50% ethanol). Absorbance was measured at 550 nm by a Sunrise™ microplate reader (Tecan, Crailsheim, Germany). For CTB assay, 5000 Jurkat cells/well were seeded into 96-well plates and on the next day were stimulated with specific concentrations of Lag A or DMSO for 72 h. Afterward, CTB reagent was added to each well for 2 h before fluorescence was determined using ex:550 nm em:595 nm by a SpectraFluor Plus™ microplate reader (Tecan, Crailsheim, Germany). Before normalization to DMSO control, day 0 values were subtracted in both experiments.

Apoptosis Assay

Cell apoptosis was detected using Nicoletti assay and Flow cytometry as described by Nicoletti et al.[11] In brief, the day before treatment, 0.1 million cells/well were seeded into 12-well plates and treated with specific concentrations of compounds or DMSO on the next day. After 24 h or 48 h, cells were harvested and washed with pre-cooled PBS. Then cells were stained with Nicoletti buffer (0.1% sodium citrate, 0.1% Triton X-100) containing 50 μg/ml PI and incubated at 4 °C for 30 min in the dark. The percentage of apoptotic cells was measured at Ex:488 nm Em:585 nm by FACSCanto II (BD, New Jersey, USA) and 10,000 events were analyzed in each sample.

Detection of ATP Production

CellTiter Glo kit was used to investigate the effect of Lag A on ATP production. 5,000 cells/well in 100 μL were plated into 96-well plates and allowed to adhere overnight. Cells were treated with subtoxic concentrations of Lag A or DMSO for 24 h and plates were equilibrated at RT for 30 min before 100 μL of CellTiter Glo reagent was added to each well. After 2 min of shaking and 10 min of incubating at RT, the values of luminescence intensity were recorded by the Tecan Sunrise microplate reader. Before normalization to DMSO control, the values of control wells containing medium without cells were subtracted.

Transmission Electron Microscopy

0.3 million cells/well were seeded into 6-well plates the night before stimulation and then treated with Lag A or DMSO for 24 h. Cells were detached and washed with PBS once before 0.45 million cells/well in each group were plated into BEEM® capsules. Subsequently, the supernatant was removed after centrifugation, and cells were incubated with 2.5% glutaraldehyde (EMS Science Services, Hatfield, PA, USA) in 0.1 M sodium cacodylate buffer (pH 7.4).

Western Blot Assay

Cells were seeded into 6-well plates at a density of 0.42 million cells/well and treated with indicated concentrations and time points of compounds or siRNA. Cells were harvested and the protein concentration was determined using a Bradford protein assay and mixed with 5× SDS sample buffer before being resolved by SDS-polyacrylamide gel electrophoresis (SDS-PAGE) and transferred to PVDF membrane. Membranes were blocked with 5% (w/v) BSA (Anprotec, cat# AC-AF-0023) in TBS-T buffer (24.8 mM Tris base, 190 mM NaCl, and 0.1% Tween-20) for 2 h at RT and subsequently incubated with appropriate primary antibodies overnight at 4 °C. The membranes were washed with TBS-T three times before incubating with HRP-conjugated secondary antibodies for 2 h at RT. After washing again with TBS-T, the chemiluminescence was visualized by incubating membranes with ECL solution (100 mM

pH 8.5 Tris, 2.5 mM Luminol, 1 mM Coumaric acid, and 17 μM H_2O_2) before using a ChemiDoc™ touch imaging system.

Immunofluorescence Staining Assay

HeLa cells were seeded inibidi8-well μ-slides (ibidi GmbH, Gräfelfing, Germany) and allowed to adhere overnight. After the corresponding treatment of compounds or DMSO, cells were washed with PBS and fixed with 4% (w/v) paraformaldehyde (PFA, Thermo Fisher Scientific, cat# 28908) in PBS for 10 min and then permeabilized with 0.5% Triton X-100 (Carl Roth, cat#3051.3) for 15 min at RT. The cells were washed with PBS and blocked in 1% (w/v) BSA in PBS for 1 h at RT followed by incubating with appropriate primary antibodies (1:200 dilution) overnight at 4 °C. On the next day, cells were washed three times with PBS containing 0.2% Triton X-100 and then incubated with Alexa fluor coupled secondary antibodies (1:400 dilution) and Hoechst 33342 (5 μg/ml) for 1 h at RT. Cells were submerged with one drop of FluorSave reagent mounting medium (Merck, cat# 345789) and covered with a glass coverslip after being washed again with PBS three times. For the MitoTracker Deep Red Staining, after treatment, cells were incubated with the pre-warmed mitotracker deep red staining solution (1:10,000 dilution) for 30 min at 37 °C incubator and washed with pre-warmed PBS. After fixation in 4% (w/v) PFA for 10 min and washed with PBS, cells were covered with FluorSave reagent mounting medium and glass coverslips. Images were captured by confocal microscopy with a Leica SP8 LSM system (Leica, Wetzlar, Germany) and the fluorescence intensity was analyzed with ImageJ software.

Mitochondrial Membrane Potential Measurement

Mitochondrial membrane potential ($\Delta\Psi m$) was determined by JC-1 staining according to the manufacturer's instructions. In detail, 0.1 million cells/well were seeded into 12-well plates overnight and stimulated with indicated concentrations of Lag A or DMSO. CCCP served as the positive control. After 24 h, cells were harvested and washed with PBS and then incubated with 1 μg/ml JC-1 working solution at 37 °C for 20 min in the dark. Subsequently, cells were washed with PBS and resuspended in PBS. The relative percentage of populations exposing red or green fluorescence was measured by FACSCanto II and 10,000 events were analyzed per sample.

Detection of Reactive Oxygen Species Release

Reactive oxygen species (ROS) release was detected using carboxy-H_2DCFDA (6-carboxy-2′,7′-dichlorodihydrofluorescein diacetate) probe staining and Flow cytometry. In brief, 0.2 million cells/well were seeded into 12-well plates the day before treatment and stimulated with indicated concentrations of Lag A or DMSO on the following day for 24 h. CCCP served as the positive control. Cells were collected by centrifugation and washed with PBS and then stained with Carboxy-H2DCFDA (10 μM) at 37 °C in the dark. After 30 min, cells were washed with PBS and resuspended in PBS followed by immediately analyzed at Ex:488 nm Em:530 nm by FACSCanto II. 10,000 events were analyzed in each sample.

Subcellular Fractionation

HeLa cells were seeded in 10 cm petri dishes overnight and on the next day were treated with different concentrations of Lag A for 24 h. According to the subcellular fractionation protocol from Abcam, cells were harvested and lysed using 500 μl of lysis buffer and then scraped immediately followed by passed through a 25 Ga needle 10 times. After incubation on ice for 20 minutes and centrifugation, the nuclear pellet and supernatant were used to further isolate the nuclear fraction and mitochondrial fraction. For nuclear fraction, the pellet was resuspended in 500 μl of lysis buffer and passed through a 25 Ga needle 10 times again. The supernatant was removed after centrifugation and the pellet was resuspended in the nuclear buffer (lysis buffer with addition 10% glycerol and 0.1% SDS) and then sonicated briefly. For mitochondrial fraction, the supernatant was centrifuged again and then the pellet was resuspended in 500 μl of lysis buffer followed by the same steps as with the nuclear pellet to get the mitochondrial fraction.

Quantification and Statistical Analysis

All repeated experiments are independent and biological replicates unless indicated otherwise. Flow cytometry data were processed with FlowJo 7.6. Confocal images and Western blot densitometry were analyzed using ImageJ. Statistical analyses were performed with GraphPad Prism 8/9. Ordinary one-way ANOVA with a post-hoc Tukey's test or Dunnett's test was performed and significance is showed as $^{ns}P > 0.12$, $*P < 0.033$, $**P < 0.002$, $***P < 0.001$. All shown graphs are presented as means ± standard error of mean (SEM). Bliss synergy score was calculated according to the Bliss independence model and the equitation is $S_{BLISS} = E_{A,B} - (E_A + E_B - E_A E_B)$, where $S_{BLISS} < 0$:antagonism, $S_{BLISS} = 0$: additive, $S_{BLISS} > 0$: synergistic.

Affinity Based Protein Profiling in Live Cells

For preparative labelling experiments in Jurkat cells, 4×10^6 cells were transferred to a 6-well plate in 2.5 ml medium w/o FBS and supplemented with the affinity-based probes at various concentrations (stock solution in DMSO, 1% final DMSO concentration). The plates were incubated for 5 hours at 37 °C, 5% CO_2 and subsequently UV-irradiated (Philips TL-D BLB 18 W UV lamps) for 10 min (except for UV-controls) while cooling on ice. Afterwards, cells were transferred to a centrifuge tube and washed with 1 ml cold PBS. Cell pellets were frozen in liquid nitrogen and stored at −80 °C until lysis. For HeLa cells, the cells were seeded on 6 cm petri dishes and grown to 90% confluence. Medium w/o FBS with the respective probe concentration (stock solution in DMSO, 1% final DMSO concentration) was prepared and 4 ml was transferred to the cells. The cells were incubated for 16 hours (37 °C, 5% CO_2), UV-irradiated (Philips TL-D BLB 18 W UV lamps) for 10 minutes and subsequently detached using a cell scraper. After washing with cold PBS the cells were frozen in liquid nitrogen and stored at −80 °C until lysis. For both cell lines pellets were thawed on ice, reconstituted in PBS with 0.4% SDS and sonicated with a sonication lance for 10 s at 60% intensity (Sonopuls HD 2070 ultrasonic rod, BANDELIN electronic GmBH & Co. KG). Cell debris was removed by centrifugation (21.000×g, 20 min) and the protein concentration of the resulting supernatant was determined using the Roti®-Quant universal kit (Carl Roth) for BCA assay. All samples were adjusted to 250 μg protein in 300 μL lysis buffer. For copper (I)-catalysed azide-alkyne cycloaddition (CuAAC), the samples were supplemented with 100 μM TBTA (1.667 mM stock in 80% tert-butanol, 20% DMSO) ligand, 200 μM biotin-azide (10 mM stock in DMSO), 1 mM $CuSO_4$ (50 mM stock in H_2O) and 1 mM TCEP (50 mM stock in H_2O) and incubated for 60 min at room temperature. The click-reaction was quenched and the proteins were precipitated by adding 5-fold excess LC–MS grade acetone and incubating at −20 °C overnight. The following day the precipitated proteins were pelleted (21.000×g, 20 min, 4 °C) and the supernatant was aspirated. To remove residual impurities, the pellet was reconstituted in 500 μL ice cold methanol by sonication (10 s, 10% intensity, Sonopuls HD

2070 ultrasonic rod, BANDELIN electronic GmBH & Co. KG) and pelleted again. The methanol was aspirated and the protein pellet was reconstituted in 500 μL 0.2% SDS in PBS by sonication (10 s, 10% intensity, Sonopuls HD 2070 ultrasonic rod, BANDELIN electronic GmBH & Co. KG). The avidin-agarose beads (Sigma-Aldrich) were equilibrated by washing 3× with 0.4% SDS in PBS and reconstituted in 0.2% SDS in PBS. 50 μL of the bead suspension was added to each sample and the samples were continuously inverted for 1 hour at room temperature to allow binding of biotin to the avidin beads. Afterwards, the beads were washed 3× with 1 mL 0.2% SDS, 2× with 1 mL 6 M urea and 3× with 1 mL PBS using centrifugation (1000×g, 3 min) and aspirating the supernatant. After washing, the beads were reconstituted in 200 μL X-buffer (7 M urea, 2 M thiourea in 20 mM HEPES buffer pH 7.5) and the proteins were reduced by the addition of 1 mM DTT (from 1 M stock in H_2O) and incubating under gentle mixing (25 °C, 950 rpm, 45 minutes). To alkylate the reduced cysteines of the proteins, 5.5 mM iodoacetamide was added (550 mM stock in 50 mM in H_2O) and incubated for 30 minutes (25 °C, 950 rpm). The alkylation reaction was quenched by adding 4 mM DTT (from 1 M stock in H_2O) and incubating for 30 minutes (25 °C, 950 rpm). The proteins were pre-digested by adding LysC (2.5 μg/mL, 0.5 mg/mL stock, FUJIFILM Wako Chemical Corporation) and incubating for 2 hours (25 °C, 950 rpm, 45 minutes). After pre-digest, 600 μL 50 mM triethlyammonium bicarbonate (TEAB) was added to each sample followed by addition 1.5 μL of Trypsin (0.5 mg/ml stock, sequencing grade, modified; Promega) for overnight digest (37 °C, 950 rpm). The following morning the digest was quenched by adding 8 μL of formic acid (FA) and the peptides were desalted using Sep-Pak C18 1 cc Vac cartridges (Waters) using the following procedure: Using gravity flow, the cartridges were first washed with 2 ml elution buffer (80% acetonitrile (MeCN), 0.5% FA) followed by washing 3× with 1 ml 0.1% TFA. The samples were now loaded and then washed 3× with 0.1% TFA and 1× with 0.5 ml 0.5% FA. The peptides were eluted from the cartridges with 2×250 μL elution buffer under gravity flow and once with 250 μL elution buffer under vacuum. The peptides were dried using a centrifugal vacuum concentrator and subsequently reconstituted in 30 μL 1% FA by placing the tubes in a sonication bath for 10 min. The peptides were then filtered using freshly equilibrated (300 μL, 1% FA) 0.22 μM Ultrafree-MC® centrifugal filters (Merck, UFC30GVNB). The filtered samples were transferred into LC–MS vials. All experiments were conducted in quadruplicates.

Affinity Based Protein Profiling in Cell Lysate

For preparative affinity based protein profiling in HeLa cell lysate, HeLa cell pellets were reconstituted in lysis buffer (1% NP-40 in PBS with cOmplete™ protease inhibitor mix, Roche) and sonicated 3×10 s (10% intensity, Sonopuls HD 2070 ultrasonic rod, BANDELIN electronic GmBH & Co. KG). The cell lysate was cleared using centrifugation (21.000×g, 4 °C, 20 min) and the protein concentration of the resulting supernatant was determined using the Roti®-Quant universal kit (Carl Roth) for BCA assay. All samples were adjusted to 500 μg protein in 500 μL lysis buffer. The affinity based probes were added at different concentrations (stock solution in DMSO, 1% final DMSO concentration) and the samples were incubated for 30 minutes at 37 °C und gentle mixing. The samples were transferred to a 48-well plate and UV-irradiated (Philips TL-D BLB 18 W UV lamps) for 10 minutes on ice. The samples were again transferred to a micro centrifuge tube and the trifunctional linker (TFL), bearing a biotin affinity tag and a rhodamine, was covalently attached using click chemistry. For this, the samples were supplemented with 100 μM TBTA (1.667 mM stock in 80% tert-butanol, 20% DMSO) ligand, 200 μM TFL (10 mM stock in DMSO), 1 mM $CuSO_4$ (50 mM stock in H_2O) and 1 mM TCEP (50 mM stock in H_2O) and incubated for 60 min at room temperature. The click-reaction was quenched and the proteins were precipitated by adding 5-fold excess LC–MS grade acetone and incubating at −20 °C overnight. The following day the precipitated proteins were pelleted (21.000×g, 20 min, 4 °C) and the supernatant was aspirated. To remove residual impurities, the pellet was reconstituted in 500 μL ice cold methanol by sonication (10 s, 10% intensity, Sonopuls HD 2070 ultrasonic rod, BANDELIN electronic GmBH & Co. KG) and pelleted again. The methanol was aspirated and the protein pellet was reconstituted in 500 μL 0.2% SDS in PBS by sonication (10 s, 10% intensity, Sonopuls HD 2070 ultrasonic rod, BANDELIN electronic GmBH & Co. KG). The avidin-agarose beads (Sigma-Aldrich) were equilibrated by washing 3× with 0.4% SDS in PBS and reconstituted in 0.2% SDS in PBS. 50 μL of the bead suspension was added to each sample and the samples were continuously inverted for 1 hour at room temperature to allow binding of biotin to the avidin beads. Afterwards, the beads were washed 3× with 1 mL 0.2% SDS, 2× with 1 mL 6 M urea and 3× with 1 mL PBS using centrifugation (1000×g, 3 min) and aspirating the supernatant. After washing, the beads were reconstituted in 200 μL X-buffer (7 M urea, 2 M thiourea in 20 mM HEPES buffer pH 7.5) and the proteins were reduced by the addition of 1 mM DTT (from 1 M stock in H_2O) and incubating under gentle mixing (25 °C, 950 rpm, 45 minutes). To alkylate the reduced cysteines of the proteins, 5.5 mM iodoacetamide was added (550 mM stock in 50 mM in H_2O) and incubated for 30 minutes (25 °C, 950 rpm). The alkylation reaction was quenched by adding 4 mM DTT (from 1 M stock in H_2O) and incubating for 30 minutes (25 °C, 950 rpm). The proteins were pre-digested by adding LysC (2.5 μg/mL, 0.5 mg/mL stock, FUJIFILM Wako Chemical Corporation) and incubating for 2 hours (25 °C, 950 rpm, 45 minutes). After pre-digest, 600 μL 50 mM triethylammonium bicarbonate (TEAB) was added to each sample followed by addition 1.5 μL of Trypsin (0.5 mg/ml stock, sequencing grade, modified; Promega) for overnight digest (37 °C, 950 rpm). The following morning the digest was quenched by adding 8 μL of formic acid (FA) and the peptides were desalted using Sep-Pak C18 1 cc Vac cartridges (Waters) using the following procedure: Using gravity flow, the cartridges were first washed with 2 ml elution buffer (80% MeCN, 0.5% FA) followed by washing 3× with 1 ml 0.1% TFA. The samples were now loaded and then washed 3× with 0.1% TFA and 1× with 0.5 ml 0.5% FA. The peptides were eluted from the cartridges with 2×250 μL elution buffer under gravity flow and once with 250 μL elution buffer under vacuum. The peptides were dried using a centrifugal vacuum concentrator and subsequently reconstituted in 30 μL 1% FA by placing the tubes in a sonication bath for 10 min. The peptides were then filtered using freshly equilibrated (300 μL, 1% FA) 0.22 μM Ultrafree-MC® centrifugal filters (Merck, UFC30GVNB). The filtered samples were transferred into LC–MS vials. All experiments were conducted in quadruplicates, at certain points during the workflow, small amounts of two samples were transferred to a micro centrifuge tube and prepared for SDS-PAGE. For this, the samples were reconstituted in Laemmli buffer.

Thermal Proteome Profiling

Thermal proteome profiling in live cells was carried out as previously reported[7a,8] with some alterations. Jurkat cells were harvested by centrifugation (5 min, 600×g) and washed with PBS. The cells where reconstituted in medium without FBS to a concentration of 4×10^6 cells/mL and 15 mL of this cell suspension were used per condition. Lagunamide A or DMSO were added to a final Lagunamide A concentration of 500 nM (0.1% final DMSO concentration). The samples were incubated in a cell culture flask for 1 h (37 °C, 5% CO_2). Upon incubation the cells were harvested (5 min, 600×g) in a falcon tube, the medium was aspirated and the

cells were reconstituted in 1.1 mL PBS with the equivalent compound or vehicle concentration. The cell suspensions were now transferred into 10 PCR tubes with 100 μL of the suspension each. The Lag A and DMSO treated samples were now subjected to a temperature gradient (37.2 °C, 41.2 °C, 45.6 °C, 49.3 °C, 52.6 °C, 54.5 °C, 57.8 °C, 60.9 °C, 64.1 °C, 67.5 °C) with each of the 10 tubes per sample representing one temperature point. After the temperature gradient the samples were incubated at 25 °C for 3 minutes before being frozen in liquid nitrogen and stored at −80 °C until lysis. To lyse the cells, they were thawed on ice, 50 μL of PBS was added and they were subjected to four freeze-thaw cycles in which they were frozen in liquid nitrogen and thawed at 25 °C. Now the samples were transferred to micro centrifuge tubes and subjected to ultra-centrifugation (20 minutes, 100.000×g, 4 °C) to remove cell debris and aggregated proteins. The protein concentration of the supernatant of the first 2 temperature points was determined using the Roti®-Quant universal kit (Carl Roth) for BCA assay. All samples were adjusted to a protein concentration of 60 μg/mL based on the average of the first 2 temperature points and the proteins were precipitated by adding a 5-fold excess of ice cold LC–MS grade acetone and incubating overnight at −20 °C. The following day the precipitated proteins were pelleted (21.000×g, 20 min, 4 °C) and the supernatant was aspirated. To remove residual impurities, the pellet was reconstituted in 500 μL ice cold methanol by sonication (10 s, 10% intensity, Sonopuls HD 2070 ultrasonic rod, BANDELIN electronic GmBH & Co. KG) and pelleted again. The methanol was aspirated and the protein pellet was reconstituted in 200 μL X-buffer (7 M urea, 2 M thiourea in 20 mM HEPES buffer pH 7.5) and the proteins were reduced by the addition of 1 mM DTT (from 1 M stock in H_2O) and incubating under gentle mixing (25 °C, 950 rpm, 45 minutes). To alkylate the reduced cysteines of the proteins, 5.5 mM iodoacetamide was added (550 mM stock in 50 mM in H_2O) and incubated for 30 minutes (25 °C, 950 rpm). The alkylation reaction was quenched by adding 4 mM DTT (from 1 M stock in H_2O) and incubating for 30 minutes (25 °C, 950 rpm). The proteins were pre-digested by adding LysC (2.5 μg/mL, 0.5 mg/mL stock, FUJIFILM Wako Chemical Corporation) and incubating for 2 hours (25 °C, 950 rpm, 45 minutes). After pre-digest, 600 μL 50 mM triethylammonium bicarbonate (TEAB) was added to each sample followed by addition 1.5 μL of Trypsin (0.5 mg/ml stock, sequencing grade, modified; Promega) for overnight digest (37 °C, 950 rpm). The following morning the digest was quenched by adding 8 μL of formic acid (FA) and the peptides were desalted using Sep-Pak C18 1 cc Vac cartridges (Waters) using the following procedure: Using gravity flow, the cartridges were first washed with 2 ml elution buffer (80% MeCN, 0.5% FA) followed by washing 3× with 1 ml 0.1% TFA. The samples were now loaded and then washed 3× with 0.1% TFA and 1× with 0.5 ml 0.5% FA. The peptides were eluted from the cartridges with 2×250 μL elution buffer under gravity flow and once with 250 μL elution buffer under vacuum. The peptides were dried using a centrifugal vacuum concentrator and subsequently reconstituted in 7.5 μL TMT-labelling buffer (50 mM HEPES, 20% MeCN, pH 8.5) through repeated vortexing, sonication (bath) and centrifugation. For TMT-labelling, 5 μL of previously prepared TMT isobaric labels (TMT10plex™ isobaric Labels Reagent set 1×0.8 mg, Thermo Fischer Scientific) were added (10 μg/μL stock concentration in anhydrous MeCN), vortexed, centrifuged and incubated for 1 h (450 rpm, 25 °C). The labelling reaction was quenched by the addition of hydroxylamine to a final concentration of 0.4%. To test whether the TMT-labelling was successful, 187.5 μL of 0.1% FA were added to each sample and 5 μL of each temperature point within a condition were combined, dried in a centrifugal vacuum concentrator, reconstituted in 1% FA and the samples were measured using LC–MS/MS. After confirming complete TMT-labelling, all temperature points within a conditions were pooled (25 μg of protein based on initial protein concentration) and dried in a centrifugal vacuum concentrator. The combined samples were now fractionated. For this, the labelled peptides were now reconstituted in 105 μL HILIC buffer A (95% MeCN, 0.1% TFA) by sonication and transferred to a LC–MS vial. The peptide fractionation was carried out using an UlitMate 3000 HPLC system (Dionex) equipped with an YMC-Pack PVA-Sil column (5 μm, 150×2.1 mm, 120 Å, YMC Europe GmbH). Gradient elution was carried out with 95% MeCN, 5% H_2O, 0.1% TFA (A) and 95% H_2O, 5% MeCN, 0.1% TFA (B). 100 μL of sample was injected and separated using a 62.5 min gradient (7.5 min 0% B, 50 min to 30% B, 3.5 min to 50% B, 2.5 min to 100% B) at a flow rate of 0.2 mL/min, followed by a washing and equilibration step. During equilibration, an on-line UV detector at 215 nm was used to monitor peptide elution. Fractions were collected into a 96-well plate and then pooled to 10 greater fractions which were dried in a centrifugal vacuum concentrator and subsequently reconstituted in 30 μL 1% FA by placing the tubes in a sonication bath for 10 min. The peptides were then filtered using freshly equilibrated (300 μL, 1% FA) 0.22 μM Ultrafree-MC® centrifugal filters (Merck, UFC30GVNB). The filtered samples were transferred into LC–MS vials. The experiment was conducted in duplicates.

Thermal Shift Assay with Purified EYA3

Cloning and purification of EYA3: The gene for EYA3 (126-573) with an N-terminal His6-sumo tag was codon-optimized for expression in *E. coli*, synthesised by *Twist Bioscience*, and cloned into pET28a vector. The vector was transformed into *E.* coli BL21-DE3 and the cells were grown in LB. The fusion-protein was expressed in BL21 DE3 (500 μM IPTG at OD_{600} of 0.6–0.8) at 18 °C for 16 hours. Cells were harvested and washed with cold PBS. Cell pellets were reconstituted in lysis buffer (50 mM Hepes pH 7.4, 200 mM NaCl, 1 mM TCEP, 10% glycerol, 1 mM PMSF, small amount of DNASE) and lysed by sonication (7 min at 30%, 3 min at 50%, 7 min at 30% intensity, Sonopuls HD 2070 ultrasonic rod, *Bandelin electronic GmbH*). The lysate was cleared at 38.000×g for 45 min and the supernatant was filtered through a 0.45 μm filter prior to purification using an Äkta Pure Protein Purification System (*Cytiva*) operated at 4 °C. Lysate was loaded onto an equilibrated 5 mL HisTrapHP column (*Cytiva*) at a flow-rate of 2 mL/min. The column was first washed with 9.5 column-volumes (CV) of 95% buffer A (50 mM Hepes pH 7.4, 200 mM NaCl, 1 mM TCEP, 10% glycerol) and 5% buffer B (50 mM Hepes pH 7.4, 250 mM NaCl, 1 mM TCEP, 10% glycerol, 500 mM imidazole) at a flow-rate of 5 mL/min and then washed with another 4 CVs of 10% buffer B. The bound proteins were eluted over a gradient of 3 CVs from 10% buffer B to 100% buffer B and another 4 CVs at 100% buffer B. The elution fractions were pooled and desalted (to remove the imidazole) using two 5 mL HiTrap desalting columns (*Cytiva*) by loading 2.5 mL of pooled fractions per run and eluting with buffer A. The resulting fractions of desalted protein was pooled and the His6-sumo tag was cleaved off by using a 1:200 ratio of sumo-protease and incubating overnight at 4 °C. The next day, an inverse His-Trap was performed with the same gradient as before. The cleaved EYA3 eluted at 5% B and was pooled and concentrated. Lastly, the protein was further purified by size-exclusion-chromatography (SEC) using a HiLoad Superdex 200 pg (*Cytiva*) using buffer A. The identity of the cleaved EYA3 was confirmed by SDS-PAGE and intact protein Mass (IP-MS).

Western blot based thermal shift assay using purified EYA3: The purified EYA3 was thawed and the buffer was exchanged to PBS to remove any glycerol from the buffer. 250 μL of protein was incubated with 50 μM Lag A, 50 μM Benzbromarone, or 1% DMSO. The samples were incubated for 30 min at 25 °C before being split into 10 PCR tubes each (25 μL per sample). The samples were incubated in a PCR cycler with a temperature gradient for

3 minutes. Each sample represents one temperature point (41 °C, 41.6 °C, 43.1 °C, 45 °C, 46.6 °C, 48.2 °C, 49.9 °C, 51.5 °C, 53.2 °C, 55 °C). Afterwards, the samples were incubated at 25 °C for 3 minutes before being placed on ice. Each sample was transferred into an ultracentrifuge tube (Beckmann Coultier) and centrifuged at 100,000×g for 20 minutes at 4 °C. The Supernatant was carefully transferred into a new micro centrifuge tube (leaving 5 μL behind to avoid agitating the precipitate). 20 μL of 2-fold Lämmli buffer was added to each sample. EYA3 was then visualized as described above in the section "Western blot". The bands corresponding to purified EYA3 were quantified using ImageJ and the background was subtracted. The values were then normalised to the average of the first two temperature points for each experiment. The graphs were prepared using Graphpad Prism 10.01 and the curves were fitted using the [inhibitor] vs. response variable slope (four parameters) curve fit function. The experiment was conducted in two independent replicates.

Mass Spectrometry for Affinity Based Protein Profiling

Photo affinity peptide samples were analyzed on an UltiMate 3000 nano HPLC system (Dionex) equipped d with an Acclaim C18 PepMap100 (75 μm ID ×2 cm) trap column and a 25 cm Aurora Series emitter column (25 cm ×75 μm ID, 1.6 μm FSC C18) (Ionoptics) separation column (column oven heated to 40 °C) coupled to an Orbitrap Fusion (Thermo Fisher) in EASY-spray setting. For peptide separation, samples were loaded on the trap column and washed for 10 min with 0.1 % TFA in ddH2O at a flow rate of 5 μL/min. Subsequently, peptides were transferred to the analytical column for peptide separation and separated using the following 132 min gradient (Buffer A: H2O + 0.1 % FA; B: MeCN + 0.1 % FA) with a flow rate of 300 nL/min.: in 7 min to 5 % B, in 105 min from 5 % to 22 %, in 10 min from 22 to 35 % and in another 10 min to 90 % B. Separation gradient was followed by a column washing step using 90 % B for 10 min and subsequent column re-equilibration with 5 % B for 5 min. MS full scans were recorded at a resolution of 120.000 with the following parameters: Ion transfer tube temperature 275 °C, RF lens amplitude 60 %, 300–1500 m/z scan range, automatic gain control (AGC) target of 2.0×10^5, 3 s cycle time and 50 ms maximal injection time. Peptides with a higher intensity than 5.0×10^3 and charge states between 2 and 7 were selected for fragmentation in the higher-energy collisional dissociation (HCD) cell at 30 % collision energy and analyzed in the ion trap using rapid scan rate. In the ion trap, the isolation window was set 1.6 m/z, an AGC target of 1.0×10^4 and a maximal injection time of 100 ms.

Mass Spectrometry for Thermal Proteome Profiling

TMT-labelled peptide samples were analyzed on an UltiMate 3000 nano HPLC system (Dionex) equipped d with an Acclaim C18 PepMap100 (75 μm ID ×2 cm) trap column and a 25 cm Aurora Series emitter column (25 cm ×75 μm ID, 1.6 μm FSC C18) (Ionoptics) separation column (column oven heated to 40 °C) coupled to an Orbitrap Fusion (Thermo Fisher) in EASY-spray setting. For peptide separation, samples were loaded on the trap column and washed for 10 min with 0.1 % TFA in ddH2O at a flow rate of 5 μL/min. Subsequently, peptides were transferred to the analytical column for peptide separation and separated using the following 120 min gradient (Buffer A: H2O + 0.1 % FA; B: MeCN + 0.1 % FA) with a flow rate of 300 nL/min.: in 10 min to 5 % B, in 50 min from 5 % to 22 % and in 60 min from 22 % to 35 %. Separation gradient was followed by a column washing step using 90 % B for 10 min and subsequent column re-equilibration with 5 % B for 5 min. MS full scans were recorded at a resolution of 120.000 with the following parameters: Ion transfer tube temperature 275 °C, RF lens amplitude 60 %, 375–1500 m/z scan range, automatic gain control (AGC) target of 2.0×10^5, 3 s cycle time and 20 ms maximal injection time. Peptides with a higher intensity than 5.0×10^3 and charge states between 2 and 7 were selected for fragmentation in the collisional induced dissociation (CID) cell at 35 % collision energy and analyzed in the ion trap using rapid scan rate. In the ion trap, the isolation window was set 1.6 m/z, an AGC target of 1.0×10^4 and a maximal injection time of 100 ms. For MS3-based reporter ion quantification, the number of synchronous precursor selection (SPS) was set to 20 with an isolation window of 2.5 m/z. The selected precursors were fragmented using the higher-energy collisional dissociation (HCD) cell at 55 % collision energy and analyzed in the orbitrap at a resolution of 60.000 with the AGC target set to 2×10^5 and a maximal injection time of 180 ms.

Data Analysis of Affinity Based Protein Profiling Experiments

MS raw data was analyzed using MaxQuant[12] software (version 1.6.17.0) and peptides were searched against Uniprot database for Homo sapiens (taxon identifier: 9606, downloaded on 04.06.2020, canonical). Carbamidomethylation of cysteines was set as fixed modification and oxidation of methionines and acetylation of N-termini were set as variable modifications. Trypsin was set as proteolytic enzyme with a maximum of 2 missed cleavages. For main search, precursor mass tolerance was set to 4.5 ppm and fragment mass tolerance to 0.5 Da. Label free quantification (LFQ) mode was activated with a LFQ minimum ratio count of 1. Second peptide identification was enabled, and false discovery rate (FDR) determination carried out by applying a decoy database and thresholds were set to 1 % FDR at peptide-spectrum match and at protein levels and "match between runs" (0.7 min match and 20 min alignment time windows) option was enabled. Normalized LFQ intensities extracted from the MaxQuant result table proteinGroups.txt were further analyzed with Perseus[13] software (version 1.6.15.0). Prior to analysis, putative contaminants, reverse hits and only identified by site hits were removed. Normalized LFQ intensities were log2 transformed and proteins with at four valid values in at least one group were used for missing value imputation from normal distribution (width 0.3, downshift 1.8, total matrix). Two-sample Students' t-test including Benjamini-Hochberg multiple testing correction (FDR = 0.05) was performed. Proteins with an enrichment factor of 2 (log2(x) = 1) and -log10 t-test p-value of 1.3 for AfBPP data and an enrichment factor of 4 (log2(x) = 2) for co-IP data and -log10 t-test pvalue of 1.31 were considered as significantly enriched proteins.

Data Analysis of Thermal Proteome Profiling Experiments

MS raw data was analysed using MaxQuant[12] software (version 1.6.17.0) and peptides were searched against Uniprot database for Homo sapiens (taxon identifier: 9606, downloaded on 04.06.2020, canonical). Carbamidomethylation of cysteines was set as fixed modification and oxidation of methionines and acetylation of N-termini were set as variable modifications. Trypsin was set as proteolytic enzyme with a maximum of 2 missed cleavages. For main search, precursor mass tolerance was set to 4.5 ppm and fragment mass tolerance to 0.5 Da. Fractions were assigned for each experiment. Group specific parameters were set to "Reporter ion MS3" with 10plex TMT isobaric labels for N-terminal and lysine modification selected. The isotope correction factor was set for each TMT channel according to the data sheet of the TMT labels. Carbamidomethylation of cysteines was set as fixed modification and oxidation of methionines and acetylation of N-termini were set as variable modifications. Trypsin was set as proteolytic enzyme

with a maximum of 2 missed cleavages. For main search, precursor mass tolerance was set to 4.5 ppm and fragment mass tolerance to 0.5 Da. Second peptide identification was enabled, and false discovery rate (FDR) determination carried out by applying a decoy database and thresholds were set to 1% FDR at peptide-spectrum match and at protein levels and "match between runs" (0.7 min match and 20 min alignment time windows) option was enabled. The remaining parameters were used as default settings. Calculated corrected reporter ion intensities were normalized to the normalized to the channel corresponding to the lowest temperature and were used to determine the melting curves of the proteins and the resulting thermal shifts (T_m). These were calculated using R (version 4.1.1) and the TPP package[7a] (version 3.20.1) using the "analyzeTPPTR" function. Proteins that fulfilled all requirements[5] were considered to have a significant thermal shift. For visualization of the TPP output files, the data was filtered as follows: $R^2 > 0.8$ for all fitted curves, plateaus < 0.3 for DMSO curves, steepest slopes of melting curves < -0.06, difference in T_m between both DMSO replicates $< 1.5\,^{\circ}C$. The resulting T_m shifts were visualized using GraphPad Prism 9.

The mass spectrometry proteomics data have been deposited to the ProteomeXchange Consortium via the PRIDE[14] partner repository with the dataset identifier PXD042129.

Synthesis of LagA Photo-Affinity Probes

All air- or moisture-sensitive reactions were carried out in oven-dried glassware (75 °C) under an atmosphere of nitrogen. Dried solvents were distilled before use: THF was distilled from sodium/benzophenone, diisopropylamine was dried with CaH_2 before distillation. Anhydrous dichloromethane, DMF, DMSO and 1,2-dimethoxyethane (DME) were purchased from Acros Organics and stored under nitrogen. Petroleum ether (40-60 °C) and ethyl acetate were distilled prior to use. The products were purified by flash chromatography on silica gel (Macherey-Nagel 60, 0.063–0.2 mm or 0.04–0.063 mm). For reversed phase flash chromatography, a Büchi Reveleris® Prep Chromatography System and Büchi FlashPure Select C18 (30 μm spherical) columns were used. Preparative HPLC was performed on a Büchi Reveleris® Prep Chromatography System using a Phenomenex Luna® C18(2) 100 Å column (250×21.1 mm, 5 μm). Analytical TLC was performed on pre-coated silica gel plates (Macherey-Nagel, Polygram® SIL G/UV_{254}). Visualization was accomplished with UV-light, ninhydrin solution, $KMnO_4$ solution or cerium(IV)/ammonium molybdate solution. Melting points were determined with a MEL-TEMP II apparatus and are uncorrected. ^1H and ^{13}C NMR spectra were recorded with Bruker Avance II 400 [400 MHz (^1H), 100 MHz (^{13}C)] or Bruker Avance I 500 [500 MHz (^1H) and 125 MHz (^{13}C)] spectrometers in $CDCl_3$, DMSO-d_6 or CD_3OD. Chemical shifts are reported in ppm (δ) with respect to TMS, and $CHCl_3$, DMSO-d_5 or methanol-d_3 was used as the internal standard. Optical rotations were measured with a Perkin Elmer Model 341 polarimeter at the sodium D line (589 nm). α_D^{20} values are given in 10^{-1} deg $cm^2\,g^{-1}$. Mass spectra were recorded with a Finnigan MAT 95 sector field spectrometer (HRMS, CI) or a Bruker Daltonics maXis 4G hr-ToF spectrometer (HRMS, ESI). Detailed methods for the synthesis can be found in the supplemental information.

Results and Discussion

Characterizing novel natural compounds, their targets, and their mode of action is one of the most challenging tasks in drug discovery, especially in the context of cancer therapy.[15] Compound supply and complicated total synthesis are the main bottlenecks for this kind of research. Chemical proteomics approaches have made target identification much easier in recent years, and we have successfully applied different techniques to identify targets of natural compounds in the past years.[6a,8,16]

Since Lag A was isolated, previous studies only focused on its structure and anti-tumor effects,[1,3] but no potential targets were investigated or proposed so far. Due to structural similarities to aurilide a pro-apoptotic effect based on mitochondrial mechanisms can be assumed. We, therefore started by investigating viability, apoptosis and mitochondria based effects of Lag A. We found that Lag A significantly inhibited cell proliferation and promoted cell apoptosis in HeLa and Jurkat cells in a nanomolar range. The half-maximal inhibitory concentration (IC50) values of Lag A against HeLa and Jurkat cells were 19.4 nM and 7.9 nM respectively (Figure 1A and 1B). As shown in Figure 1C and 1D, the percentage of apoptotic cells was increased by Lag A stimulation in both cell lines compared to the DMSO control and the concentrations for 50% of maximal effect (EC50) of Lag A against HeLa and Jurkat cells were 40.5 and 5.6 nM respectively. These data show that Lag A exerts its potent anti-tumor effect by affecting cell proliferation and cell apoptosis.

Since aurilide, a natural compound, which is structurally closely related to Lag A (Figure 2) has been demonstrated to elicit its cellular effects (e.g. promotion of apoptosis) via alteration of mitochondrial function,[5] and since a mitochondrial

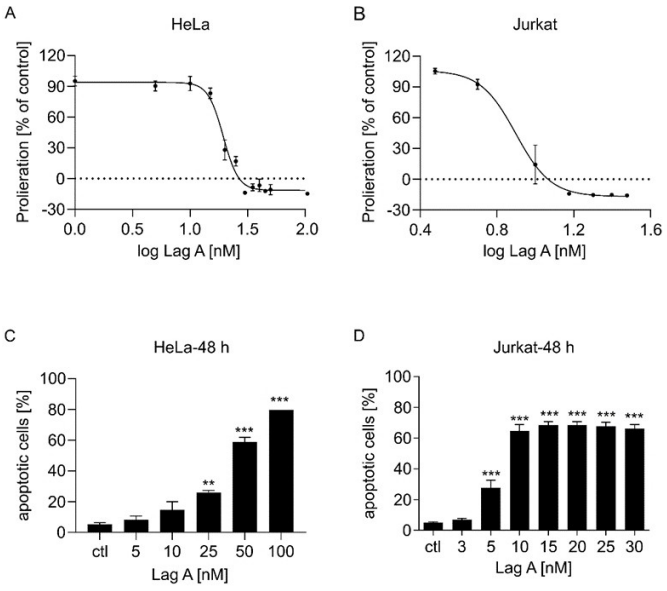

Figure 1. Lag A inhibits cell proliferation and promotes cell apoptosis in HeLa and Jurkat cells. (A) Effect of Lag A on cell proliferation in HeLa cells was measured by crystal violet staining assay after indicated treatment for 72 h. The percentage of cells was normalized to DMSO control. Data are plotted as the means ± SEM, n = 3. (B) Effect of Lag A on cell proliferation in Jurkat cells was measured by CTB assay (since the crystal violet assay is not applicable for suspension cells) after indicated treatment for 72 h. Data are presented as means ± SEM, n = 3. (C) Effect of Lag A on cell apoptosis in HeLa cells was detected by Nicoletti assay after treatment with different concentrations for 48 h. Data are presented as means ± SEM, n = 3, one-way ANOVA, Dunnett's test, $^{**}P < 0.002$, $^{***}P < 0.001$. (D) As in (C), except the cell line is Jurkat cells.Main Text Paragraph.

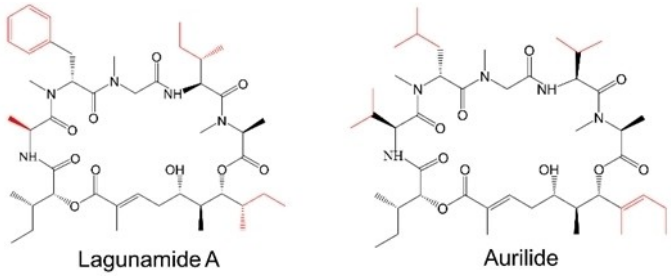

Figure 2. Lagunamide A and aurilide are structurally similar. Structural differences are highlighted in red.

target (prohibitin) has been identified for this compound in an affinity based approach,[5] we also investigated mitochondrial effects of Lag A.

By utilizing transmission electron microscopy (TEM) we were able to see a clear change of mitochondrial morphology after Lag A treatment. The mitochondrial morphology in the control group showed a structurally intact outer membrane and clearly visible cristae structure while mitochondria became significantly smaller with a highly condensed matrix after treatment with Lag A (Figure 3A). Moreover, to confirm this change, HeLa cells were stained with MitoTracker™ deep red and subsequently

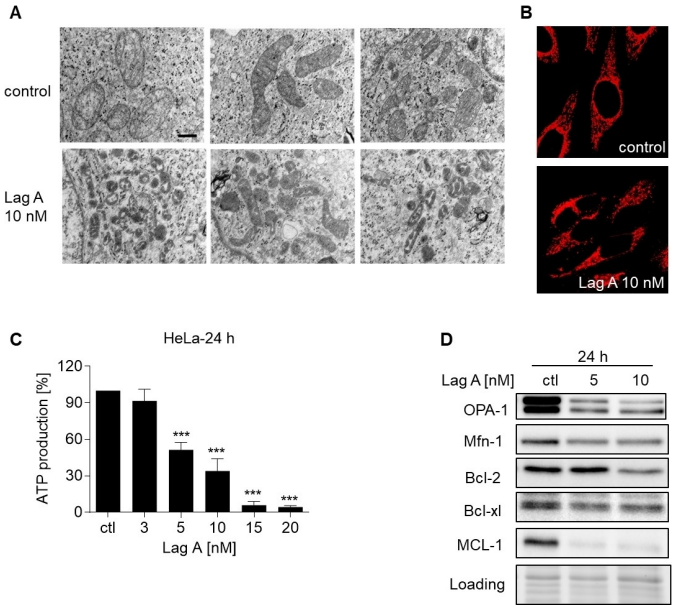

Figure 3. Lag A causes severe mitochondrial dysfunction. (A and B) Mitochondrial morphology alterations were detected using Transmission electron microscopy (A) and mitotracker deep red staining (B) in 24 h Lag A treated-cells. Representative images are from one of three independent experiments. Scale bar represents 500 nm and 10 μm for (A) and (B) respectively. Quantitative analysis of the data in (A) and (B) can be found in Supplementary Figure S2 A. (C) ATP production measurement using CellTiter Glo kit, following 24 h of indicated treatment with Lag A. Culture medium values were subtracted as blanks from each well and the percentages of ATP production were normalized to DMSO control. The values are means ± SEM, n = 3 (one-way ANOVA, Dunnett's test, ***$P < 0.001$). (D) Western blot of mitochondrial related proteins, including OPA-1, Mfn-1, Bcl-2, Bcl-xl and Mcl-1 after 24 h of treatment with Lag A. Representative image of three independent experiments. Further images are given in Supplementary Figure S3).

confocal microscopy was applied. As expected, Lag A caused similar mitochondrial morphological alteration with fragmentation of mitochondria and increased fission compared to the DMSO control (Figure 3B).

Based on this change, we further investigated the effect of Lag A on mitochondrial function. As shown in Figure 3C, subtoxic concentrations of Lag A led to robust reduction in the ratio of ATP production compared to the DMSO control. Besides, Lag A also induced a dramatic drop in mitochondrial membrane potential (MMP, $\Delta\Psi m$) (Supplementary Figure S1A and B), which is another key indicator of mitochondrial activity and influences the production of ATP (Figure 3C) as well as reactive oxygen species (ROS). ROS were elevated in both HeLa and Jurkat cells (Supplementary Figure S2B). In view of the alteration in mitochondrial morphology and function after Lag A treatment, key mitochondrial related proteins were evaluated. As shown in Figure 3D, notably, OPA-1 and Mfn-1, important proteins for maintaining mitochondrial fusion and fission,[17] were clearly reduced by Lag A treatment, which is consistent with the mitochondrial morphological alteration. Lag A markedly down-regulated the expression levels of the anti-apoptotic Bcl-2 family proteins including Bcl-2, Bcl-xl and Mcl-1. In addition, to decipher whether Lag A promotes cell apoptosis through the mitochondrial pathway, cytochrome c release from mitochondria was detected using subcellular fractionation after Lag A treatment. Lag A caused a significant reduction of cytochrome c from mitochondria accompanied with an increase of the protein in the cytosolic fraction (Supplementary Figure S2C).

To identify the mitochondrial protein targets of Lag A in anlogy to aurilide, we initially synthesized an affinity based probe (OA725-2) bearing a photo crosslinking moiety for covalent binding to the target proteins and an alkyne moiety for attachment of an enrichment handle (Supplementary Figure S4A) via copper catalyzed azide alkyne cycloaddition (CuAAC).[18] As the natural product Lag A bears a phenyl moiety the most straight forward way to introduce a photo cross linker was to convert the phenyl ring to an aryl-azide moiety. The alkyne moiety was introduced via an ether adjacent to the macrolacton ester. As in our previously reported synthesis of Lag A,[19] we built up the stereocenters of the modified polyketide part via iterative Matteson homologations (SI synthesis route and Supplementary Figure S4A,). The potency of the photo affinity probe concerning anti-proliferative action was reduced by approx. a factor of 200 as compared to Lag A (Figure 1A and B and Figure S4A), nevertheless it was still active in the nanomolar concentration range, which encouraged us to go ahead with proteomic studies in living cells. Surprisingly, the new probes were only taken up slowly, necessitating long incubation times (data not shown). After labelling, CuAAC to biotin-azide, enrichment using avidin beads tryptic digest and LC–MS/MS no reproducibly enriched protein targets were detected. To overcome the slow uptake, we also performed these experiments in cell lysate (Supplementary Figure S4B) which also did not reveal any enriched proteins. The affinity-based probe was therefore not suitable for target identification of Lag A. Due to synthetic reasons we had to place the position

for the linker in the Lag A probe at a different position in comparison to the published aurilide probe.[5] This might explain why we were not able to identify a target protein, though the functional data (e.g. mitochondrial morphology, ATP production, oxygen consumption rate) also clearly point towards a mitochondrial target of Lag A. This also demonstrates that label based approaches, and the related changes of the structure of the compound of interest can severely restrict the applicability of this approach.

To overcome these limitations, we performed TPP using the natural product Lag A. Jurkat cells were treated in situ with 500 nM Lag A or vehicle control and were exposed to a temperature gradient. After lysis and isolation of the soluble fraction by ultracentrifugation, the proteomes were digested and subsequently labeled with tandem mass tags (TMT). After labelling the different temperature points with different TMT-channels, the 10 temperature points were combined and then fractionated by hydrophilic interaction chromatography (HILIC). The fractions were analyzed by LC–MS/MS/MS (Figure 4A). The T_m shifts were calculated for both replicates and plotted after filtering (Figure 4B, see Methods section for filtering criteria). In addition to comparing the Tm shifts, a non-parametric spline-based test was conducted for more robust statistical analysis.[20] Four proteins were stabilized by more than 2.5 °C in both Lag A treated samples and passed all additional significance thresholds, while three proteins were destabilized by more than 2.5 °C and passed all additional significance thresholds (Proteins marked in blue in Figure 4B and Supplementary Table S2). The three destabilized proteins (RPL30, RPL10A, MRPL46) are all components of the large ribosomal subunit. Destabilization of the ribosomal complex is an effect that we often see in a large variety of TPP analysis. The exact reason for this is still under investigation, and is probably linked to general stress response. Among the four stabilized proteins were EYA3 (eyes absent homolog 3), SMC1A (Structural maintenance of chromosomes protein 1 A) and NDC80 (Kinetochore Protein NDC80 Homolog). EYA3 and SMC1A both play a role in DNA damage repair, while NDC80 organizes and stabilizes microtubule-kinetochore interactions. NDC80 and SMC1A have in common that they are required for proper chromosome segregation.[21] The fourth protein, GCFC2 (also known as C2ORF3) is presumably a transcriptional regulator, which seems to be associated with dyslexia[22] The melting curves of the stabilized protein EYA3 showed pronounced stabilization of 4 °C or more in both biological replicates (Figure 4C).

Among the potential targets of Lag A, EYA3, a protein that is essential for the DNA damage repair process,[23] was selected for validation due to its crucial role in apoptosis and survival decision of cells.[24] Here, doxorubicin (DXR), a widely used chemotherapeutic drug and DNA damaging agent,[25] was chosen to establish DNA damage. DNA damage repair is crucial to maintain cell survival and genomic stability,[26] which is an

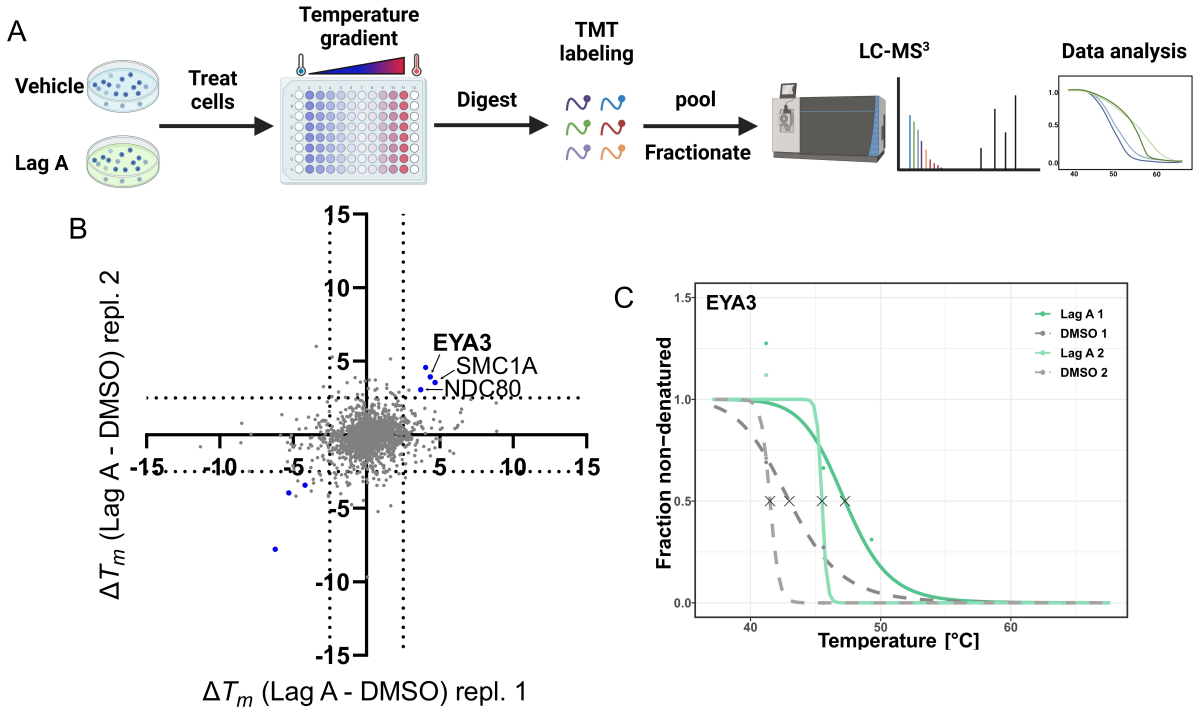

Figure 4. Target Identification of Lag A using thermal protein profiling. (A) Schematic workflow of the thermal proteome profiling experiment. Living Jurkat cells were treated with 500 nM of Lag A or DMSO for 1 hour. Subsequently, aliquots were incubated at 10 different temperatures ranging from 37 °C to 67 °C. After isolating the soluble fraction via centrifugation, the proteins were digested and TMT labelled before being fractionated and analysed by mass spectrometry. (B) Scatter plot of the calculated thermal shifts (△Tm) between vehicle and Lag A treated cells. Proteins that have passed all significance criteria (see methods) are displayed in blue. Samples were measured using MS3 based reporter ion quantification and raw data was analysed using MaxQuant.[12] Thermal response curve fitting as well as melting points were calculated using the TPP R package. (C) Thermal response curve of target protein EYA3. Lag A treated samples are displayed in green while Vehicle treated samples are displayed in grey. The melting points (Tm) are marked by a X.

important hallmark of cancer drivers.[27] Once DNA damage is caused by genetic stress or certain chemotherapeutics (like e.g. doxorubicin, which we used), cancer cells will induce the DNA damage repair process, and may keep proliferating and surviving under an adequate DNA damage repair. To monitor the DNA damage and repair process, the change of γH2AX (phosphorylation of histone H2AX at Ser139), an early cellular response to the induction of DNA double-strand breaks, was selected as a marker.[28] In order to detect the effect of Lag A on the DNA damage repair process, immunofluorescence staining was used. As expected, DXR treatment induced a strong increase of γH2AX intensity, whereas there was no significant increase in fluorescence signal of γH2AX when the cells were pre-treated with Lag A prior to DXR treatment (Figure 5A). To confirm the phenotype, the relative protein level of γH2AX was investigated using western blot. In good accordance with the staining results, the level of γH2AX was increased significantly upon DXR treatment, while a Lag A combination treatment with DXR resulted in significantly reduced expression levels of γH2AX (Figure 5B). It is a widely accepted concept that after DNA damage, cells need to decide, whether DNA repair is possible, or whether they are beyond repair and should undergo apoptosis.[29] Therefore, we next examined, whether Lag A influences this decision and acts synergistically with DXR on cell apoptosis. HeLa cells showed a significant increase of the percentage of apoptotic cells in response to treatment with a subtoxic dose of Lag A in combination with DXR compared to Lag A or DXR treatment alone (Figure 5C). The Bliss scores calculated according to Bliss independence model were over 1 (Table S1). This indicates the synergistic effect of Lag A in combination with DXR. Thus, HeLa cells pre-treated with Lag A were more sensitive to DXR-induced DNA damage.

To investigate, whether EYA3 is functionally responsible for the effect of Lag A on DNA damage repair, a genetic knockdown was used. As shown in Figure 5D, the effect of Lag A on the formation of DNA repair foci (γH2AX intensity) after treatment with DXR, was inhibited significantly after EYA3 knockdown (KD). Moreover, to further confirm this effect, Western blot was conducted using the same conditions as for imaging. As expected, the γH2AX in the cells treated with Lag A and DXR combination was elevated in EYA3 KD cells compared to NT control cells (Figure 5E). Both results substantiate that EYA3 silencing overrides the effect of Lag A on inhibiting the formation of DNA damage repair foci after treatment with DXR, and indicate EYA3 as functionally important for the effects of of Lag A. To test, whether EYA3 is indeed a direct target of Lag A, we performed a CETSA experiment with recombinantly expressed and purified EYA3 protein. Surprisingly, Lag A did not increase thermal stability of EYA3, while 6-hydroxybenzbromarone, a well-established inhibitor of EYA3, did (Supplementary Figure S6). This inconsistency to the TPP data from whole cells indicates that Lag A treatment indirectly stabilizes EYA3 via modulating some posttranslational modification, protein-protein interaction, or its intracellular localization.[9–10] While Lag A does not seem to directly bind EYA3, the downstream stabilization observed in the cellular TPP experiment gave the impetus to investigate its role in the mechanism of action.

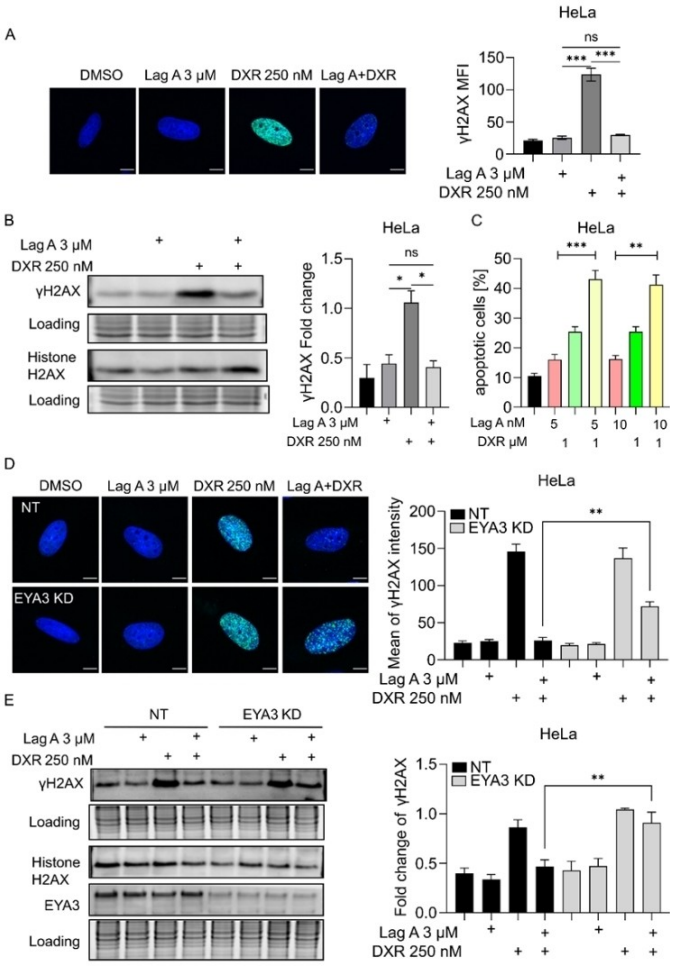

Figure 5. Lag A inhibits formation of DNA damage repair foci after treatment with doxorubicin via interaction with EYA3. (A) Left: Immunofluorescence images of γH2AX (green)and Hoechst 33342 as nuclear counter stain (blue) in treated HeLa cells. Cells were pre-treated with 3 μM Lag A for 1 h before 250 nM DXR was added for another 2 h and then medium was changed into fresh medium for 1 h. Right: Bar graph shows the mean fluorescence intensity of γH2AX from three independent experiments using ImageJ and at least 70 cells were collected in each group for quantitative analysis. The values are means ± SEM, n = 3 (one-way ANOVA, Tukey's test, nsp > 0.12, *** $P < 0.001$). Scale bar represents 10 μM. (B) Left: Western blot of γH2AX and Histone H2AX after treatments as described in (A). The shown images are from one of three independent replicates. Right: Immunoblot quantification of γH2AX expression level normalized to Histone H2AX using ImageJ. (Data are presented as means ± SEM, n = 3, one-way ANOVA, Tukey's test, nsp > 0.12, ** $P < 0.002$). (C) Effect of Lag A on DXR-induced cell apoptosis was determined by Nicoletti assay. HeLa cells were treated with indicated concentrations of Lag A for 24 h followed by stimulation with DXR for another 24 h. Error bars represent SEM, n = 3, one-way ANOVA, Tukey's test, **$P < 0.002$, ***$P < 0.001$. (D) Left: As in (A), except HeLa cells were transfected with NT siRNA or EYA3 siRNA for 24 h prior to indicated compounds treatment. Right: Quantification of γH2AX fluorescence intensity using ImageJ. At least 70 cells were collected in each group for quantitative analysis and data are presented as means ± SEM, n = 3, one-way ANOVA, Tukey's test, **$P < 0.002$. Scale bar: 10 μM. (E) Left: As in (B), except HeLa cells were transfected with NT siRNA or EYA3 siRNA for 24 h prior to indicated compounds treatment. Right: Immunoblot quantification of γH2AX expression level normalized to Histone H2AX using ImageJ (Data are presented as means ± SEM, n = 3, one-way ANOVA, Tukey's test, **$P < 0.002$).

EYA3 belongs to the Eye Absent (EYA) family. EYA family members contain the N-terminal transactivation domain and

the C-terminal tyrosine phosphatase domain, enabling them to act as transcriptional activators and tyrosine phosphatases.[30] This phosphatase functionality (dephosphorylation of the Tyr139 residue in H2AX) has previously been described as essential for the role of EYA3 in the formation of DNA repair complexes.[24] Since we did not detect changes of this phosphorylation site upon treatment with Lag A (Supplementary Figure S5C), we assume that the effects we observe are independent of this phosphatase activity. Our results hint towards an as of yet unknown role of EYA3 in the DNA-damage response mechanism which is independent of the dephosphorylation of H2AX Tyr142.

Interestingly, we found that EYA3 KD did as such not affect cell apoptosis and cell proliferation in HeLa cells (Supplementary Figure S5A and B), which is contradictory to a role for EYA3 in cell proliferation as previously reported.[31] This may be caused by cell-type specific effects of the silencing approach, or by the EYA3 levels remaining after knockdown.

Chemotherapy resistance is an urgent issue for clinical treatment.[32] Since EYA proteins are over-expressed in different cancer cell lines, including breast cancers,[31] Ewing sarcoma,[33] and lung cancers,[34] it might be a promising approach to design and investigate natural products and small molecules that modulate the biological activity of these proteins.

Conclusions

Our work shows the complexity of proteomic based techniques for drug target identification, due to limitations of label based approaches, as well as the potential pitfalls of TPP. We were not able to identify a target for the observed mitochondrial effects of Lag A, which might be the cause of previously described cytotoxic effects of this compound.[1,4] While we were not able to identify the direct targets of Lag A using AfBPP or TPP, the holistic nature of TPP in live cells, did enable us to identify downstream cellular effects of Lag A. We could show that EYA3, while not being directly targeted by Lag A, plays an important role in the modulation of the DNA damage response. This work proposes an intriguing new mechanism of action in which Lag A treatment tips the balance of DNA damage response towards more apoptosis, although this is probably not the only mechanism. This work therefore highlights the utility of unbiased proteomic approaches in elucidating complex mechanisms of action in live cells, whether by identifying the direct targets of a drug, or by providing insights into downstream effects.

Supporting Information

Additional supporting information can be found online in the Supporting Information section at the end of this article.

Acknowledgements

The authors gratefully acknowledge financial supply to Y.H. by the Chinese Scholarship Council (CSC). SAS acknowledges funding by the Merck Future Insight Prize 2020. We would like to thank Dr. Sabine Schmitt and Carola Eberhagen for doing electron microscopy analyses. Open Access funding enabled and organized by Projekt DEAL.

Conflict of Interests

The authors declare no conflict of interest.

Data Availability Statement

The data that support the findings of this study are available from the corresponding author upon reasonable request.

Keywords: Lagunamide A · TPP · thermal protein profiling · Affinity based protein profiling · DNA damage

[1] A. Tripathi, J. Puddick, M. R. Prinsep, M. Rottmann, L. T. Tan, *J. Nat. Prod.* **2010**, *73*, 1810–1814.
[2] S. Michon, F. Cavelier, X. J. Salom-Roig, *Mar. Drugs* **2021**, *19*.
[3] A. Tripathi, W. Fang, D. T. Leong, L. T. Tan, *Mar. Drugs* **2012**, *10*, 1126–1137.
[4] X. Huang, W. Huang, L. Li, X. Sun, S. Song, Q. Xu, L. Zhang, B. G. Wei, X. Deng, *Mol. Pharm.* **2016**, *13*, 3756–3763.
[5] S. Sato, A. Murata, T. Orihara, T. Shirakawa, K. Suenaga, H. Kigoshi, M. Uesugi, *Chem. Biol.* **2011**, *18*, 131–139.
[6] a) C. M. Gleissner, C. L. Pyka, W. Heydenreuter, T. F. Gronauer, C. Atzberger, V. S. Korotkov, W. Cheng, S. M. Hacker, A. M. Vollmar, S. Braig, S. A. Sieber, *ACS Cent. Sci.* **2019**, *5*, 1170–1178; b) D. K. Nomura, M. M. Dix, B. F. Cravatt, *Nat. Rev. Cancer* **2010**, *10*, 630–638; c) L. E. Sanman, M. Bogyo, *Annu. Rev. Biochem.* **2014**, *83*, 249–273.
[7] a) H. Franken, T. Mathieson, D. Childs, G. M. Sweetman, T. Werner, I. Togel, C. Doce, S. Gade, M. Bantscheff, G. Drewes, F. B. Reinhard, W. Huber, M. M. Savitski, *Nat. Protoc.* **2015**, *10*, 1567–1593; b) J. Perrin, T. Werner, N. Kurzawa, A. Rutkowska, D. D. Childs, M. Kalxdorf, D. Poeckel, E. Stonehouse, K. Strohmer, B. Heller, D. W. Thomson, J. Krause, I. Becher, H. C. Eberl, J. Vappiani, D. C. Sevin, C. E. Rau, H. Franken, W. Huber, M. Faelth-Savitski, M. M. Savitski, M. Bantscheff, G. Bergamini, *Nat. Biotechnol.* **2020**, *38*, 303–308; c) M. M. Savitski, F. B. Reinhard, H. Franken, T. Werner, M. F. Savitski, D. Eberhard, D. Martinez Molina, R. Jafari, R. B. Dovega, S. Klaeger, B. Kuster, P. Nordlund, M. Bantscheff, G. Drewes, *Science* **2014**, *346*, 1255784.
[8] V. C. Kirsch, C. Orgler, S. Braig, I. Jeremias, D. Auerbach, R. Muller, A. M. Vollmar, S. A. Sieber, *Angew. Chem. Int. Ed. Engl.* **2020**, *59*, 1595–1600.
[9] C. S. H. Tan, K. D. Go, X. Bisteau, L. Dai, C. H. Yong, N. Prabhu, M. B. Ozturk, Y. T. Lim, L. Sreekumar, J. Lengqvist, V. Tergaonkar, P. Kaldis, R. M. Sobota, P. Nordlund, *Science* **2018**, *359*, 1170–1177.
[10] J. X. Huang, G. Lee, K. E. Cavanaugh, J. W. Chang, M. L. Gardel, R. E. Moellering, *Nat. Methods* **2019**, *16*, 894–901.
[11] C. Riccardi, I. Nicoletti, *Nat. Protoc.* **2006**, *1*, 1458–1461.
[12] J. Cox, M. Mann, *Nat. Biotechnol.* **2008**, *26*, 1367–1372.
[13] S. Tyanova, T. Temu, P. Sinitcyn, A. Carlson, M. Y. Hein, T. Geiger, M. Mann, J. Cox, *Nat. Methods* **2016**, *13*, 731–740.
[14] Y. Perez-Riverol, J. Bai, C. Bandla, D. Garcia-Seisdedos, S. Hewapathirana, S. Kamatchinathan, D. J. Kundu, A. Prakash, A. Frericks-Zipper, M. Eisenacher, M. Walzer, S. Wang, A. Brazma, J. A. Vizcaino, *Nucleic Acids Res.* **2022**, *50*, D543–D552.
[15] G. M. Cragg, P. G. Grothaus, D. J. Newman, *Chem. Rev.* **2009**, *109*, 3012–3043.
[16] a) M. A. Carnero Corrales, S. Zinken, G. Konstantinidis, M. Rafehi, A. Abdelrahman, Y. W. Wu, P. Janning, C. E. Muller, L. Laraia, H. Waldmann,

Cell Chem. Biol. **2021**, *28*, 1750–1757e1755; b) F. Koczian, O. Naglo, J. Vomacka, B. Vick, P. Servatius, T. Zisis, B. Hettich, U. Kazmaier, S. A. Sieber, I. Jeremias, S. Zahler, S. Braig, *Haematologica* **2019**, *104*, 546–555; c) P. Le, M. B. Nodwell, J. Eirich, S. A. Sieber, *Chemistry* **2019**, *25*, 12644–12651; d) T. Reinhardt, K. M. Lee, L. Niederegger, C. R. Hess, S. A. Sieber, *ACS Chem. Biol.* **2022**, *17*, 3077–3085.
[17] H. M. McBride, M. Neuspiel, S. Wasiak, *Curr. Biol.* **2006**, *16*, R551–560.
[18] a) V. V. Rostovtsev, L. G. Green, V. V. Fokin, K. B. Sharpless, *Angew. Chem. Int. Ed. Engl.* **2002**, *41*, 2596–2599; b) C. W. Tornoe, C. Christensen, M. Meldal, *J. Org. Chem.* **2002**, *67*, 3057–3064.
[19] J. Gorges, U. Kazmaier, *Org. Lett.* **2018**, *20*, 2033–2036.
[20] D. Childs, K. Bach, H. Franken, S. Anders, N. Kurzawa, M. Bantscheff, M. M. Savitski, W. Huber, *Mol. Cell. Proteomics* **2019**, *18*, 2506–2515.
[21] a) I. M. Cheeseman, A. Desai, *Nat. Rev. Mol. Cell Biol.* **2008**, *9*, 33–46; b) F. Yi, Y. Zhang, Z. Wang, Z. Wang, Z. Li, T. Zhou, H. Xu, J. Liu, B. Jiang, X. Li, L. Wang, N. Bai, Q. Guo, Y. Guan, Y. Feng, Z. Mao, G. Fan, S. Zhang, C. Wang, L. Cao, B. P. O'Rourke, Y. Wang, Y. Wu, B. Wu, S. You, N. Zhang, J. Guan, X. Song, Y. Sun, S. Wei, L. Cao, *Sci. Adv.* **2021**, *7*.
[22] a) L. Beguinot, H. Yamazaki, I. Pastan, A. C. Johnson, *Cell Growth Differ.* **1995**, *6*, 699–706; b) H. Matsson, M. Huss, H. Persson, E. Einarsdottir, E. Tiraboschi, J. Nopola-Hemmi, J. Schumacher, N. Neuhoff, A. Warnke, H. Lyytinen, G. Schulte-Korne, M. M. Nothen, P. H. Leppanen, M. Peyrard-Janvid, J. Kere, *J. Hum. Genet.* **2015**, *60*, 399–401.
[23] N. Krishnan, D. G. Jeong, S. K. Jung, S. E. Ryu, A. Xiao, C. D. Allis, S. J. Kim, N. K. Tonks, *J. Biol. Chem.* **2009**, *284*, 16066–16070.
[24] P. J. Cook, B. G. Ju, F. Telese, X. Wang, C. K. Glass, M. G. Rosenfeld, *Nature* **2009**, *458*, 591–596.
[25] K. M. Tewey, T. C. Rowe, L. Yang, B. D. Halligan, L. F. Liu, *Science* **1984**, *226*, 466–468.
[26] M. Shrivastav, L. P. De Haro, J. A. Nickoloff, *Cell Res* **2008**, *18*, 134–147.
[27] D. Hanahan, *Cancer Dis.* **2022**, *12*, 31–46.
[28] L. J. Mah, A. El-Osta, T. C. Karagiannis, *Leukemia* **2010**, *24*, 679–686.
[29] W. P. Roos, A. D. Thomas, B. Kaina, *Nat. Rev. Cancer* **2016**, *16*, 20–33.
[30] a) J. P. Rayapureddi, C. Kattamuri, B. D. Steinmetz, B. J. Frankfort, E. J. Ostrin, G. Mardon, R. S. Hegde, *Nature* **2003**, *426*, 295–298; b) X. Li, K. A. Oghi, J. Zhang, A. Krones, K. T. Bush, C. K. Glass, S. K. Nigam, A. K. Aggarwal, R. Maas, D. W. Rose, M. G. Rosenfeld, *Nature* **2003**, *426*, 247–254; c) L. Zhang, H. Zhou, X. Li, R. L. Vartuli, M. Rowse, Y. Xing, P. Rudra, D. Ghosh, R. Zhao, H. L. Ford, *Nat. Commun.* **2018**, *9*, 1047.
[31] R. N. Pandey, R. Rani, E. J. Yeo, M. Spencer, S. Hu, R. A. Lang, R. S. Hegde, *Oncogene* **2010**, *29*, 3715–3722.
[32] a) M. R. Middleton, G. P. Margison, *Lancet Oncol.* **2003**, *4*, 37–44; b) D. B. Zamble, S. J. Lippard, *Trends Biochem. Sci.* **1995**, *20*, 435–439.
[33] Y. Wang, R. N. Pandey, K. Roychoudhury, D. Milewski, T. V. Kalin, S. Szabo, J. G. Pressey, R. S. Hegde, *Mol. Cancer Ther.* **2021**, *20*, 803–815.
[34] Z. Li, R. Qiu, X. Qiu, T. Tian, *Oncotarget* **2017**, *8*, 110837–110848.

Manuscript received: January 9, 2024
Revised manuscript received: May 6, 2024
Accepted manuscript online: May 8, 2024
Version of record online: ■■, ■■

RESEARCH ARTICLE

Using TPP (Thermal Proteome Profiling) we identify EYA3 as component of the molecular mode of action of the natural compound Lagunamide A (Lag A). Lag A targeting the DNA damage repair process sets a promising starting point to study basic chemotherapy resistance mechanisms and to develop more effective chemo-sensitizing drugs.

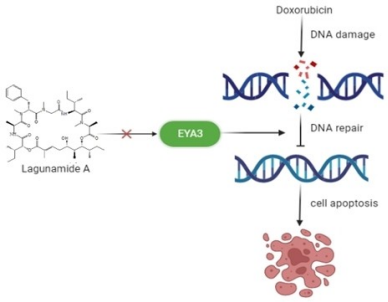

Dr. Y. Hu, D. Mostert, Dr. C. Orgler, Dr. O. Andler, Prof. H. Zischka, Prof. U. Kazmaier, Prof. A. M. Vollmar, Dr. S. Braig, Prof. S. A. Sieber, Prof. S. Zahler**

1 – 13

Thermal Proteome Profiling Reveals Insight to Antiproliferative and Pro-Apoptotic Effects of Lagunamide A in the Modulation of DNA Damage Repair